Research Article

Journal of PeptideScience

Received: 17 May 2010 Revised: 22 July 2010 Accepted: 30 July 2010 Published online in Wiley Online Library: 2 September 2010

(wileyonlinelibrary.com) DOI 10.1002/psc.1289

Nanopore analysis of tethered peptides

Howard Meng, Dielle Detillieux, Christian Baran, Besnik Krasniqi, Christopher Christensen, Claudia Madampage, Radu I. Stefureac and Jeremy S. Lee*

Peptides of 12 amino acids were tethered via a terminal cysteine to mono-, di-, tri-, and tetrabromomethyl-substituted benzene to produce bundles of one to four peptide strands (CY12-T1 to CY12-T4, respectively). The interaction of the bundles with the α-hemolysin pore was assessed by measuring the blockade currents (*I*) and times (*T*) at an applied potential of −50, −100, and −150 mV. Three types of events could be distinguished: bumping events, with small *I* and short *T* where the molecule transiently interacts with the pore before diffusing away; translocation events, where the molecule threads through the pore with large *I* and the value of *T* decreases with increasing voltage; and intercalation events, where the molecule transiently enters the pore but does not translocate with large *I* and the value of *T* increases with increasing voltage. CY12-T1 and CY12-T2 gave only bumping and translocation events; CY12-T3 and CY12-T4 also gave intercalation events, some of which were of very long duration. The results suggest that three uncoiled peptide strands cannot simultaneously thread through the α-hemolysin pore and that proteins must completely unfold in order to translocate.

Supporting information may be found in the online version of this article

Keywords: α-hemolysin; nanopore; tethered peptides; translocation; intercalation

Introduction

Nanopores such as α-hemolysin are bacterial toxins that self-assemble into lipid membranes and allow the facile translocation of small molecules [1,2]. In nanopore analysis, a voltage is applied across the pore which produces a current in the pA range due to ionic conductance [3–6]. If a molecule enters the pore, a blockade current, *I*, will be observed for a blockade time, *T*, the values of *I* and *T* being dependent on the structure and charge of individual molecules (Figure 1). Originally, this technique was applied to the study of nucleic acids and recently significant progress has been made toward achieving rapid DNA sequencing [7–15]. Peptides and small proteins can also be studied, although sequencing will be more challenging because of the problem of distinguishing 20 amino acids rather than just 4 nucleic acid bases. On the other hand, the opening in the α-hemolysin pore is only 1.5 nm, so that even small proteins such as a Zn-finger must unfold in order to translocate [16–18]. Thus, nanopore analysis is a promising technique for studying the folding of individual protein molecules.

For most small peptides, translocation appears to be eminently reasonable especially given the similarities to the events observed for DNA and RNA [19–26]. Thus, for many peptides, a histogram of current blockades shows two Gaussian distributions; one centered at 20–30% of the open pore current which is assigned to bumping events, and the second at 50–100% which represents putative translocations. Indirect evidence for translocation includes (i) an increase in *T* with the length of peptide, but there are exceptions if the peptide folds up or sequence effects may predominate [21–23]; (ii) a decrease in *T* with an increase in voltage, but this may only apply to peptides which are electrophoretically driven through the pore (i.e. a negatively charged peptide with the positive electrode on the *trans* side [20]); and (iii) a change in *T* when amino acid residues at either the *cis* entrance or *trans* exit of the pore are modified due to the interaction of the peptide with the inside of the pore [24]. The latter is perhaps the most compelling.

Translocation of proteins is more challenging to understand because they must unfold in order to thread through the pore [16–18,27,28]. In our laboratory, most proteins also give two peaks in the event histogram of current blockades (to be published elsewhere); so it is tempting to assign the peak with the smaller value of *I* to the interaction of the protein with the outside of the pore i.e. bumping events (Figure 1A), and the peak with the highest current blockade would be due to translocation events (Figure 1C). However, it is also possible that the protein (or a loop or a domain) may become transiently stuck in the vestibule of the pore before diffusing away (Figure 1B). We propose to call this an intercalation event by analogy with the intercalation of drugs into DNA [29]. Such an event would have a large value of *I* and would be very difficult to distinguish from a putative translocation. It might be argued that the value of *T* would increase with increasing applied

* *Correspondence to: Jeremy S. Lee, Department of Biochemistry, 107 Wiggins Road, University of Saskatchewan, SK, Canada S7N 5E5.*
E-mail: jeremy.lee@usask.ca

Department of Biochemistry, 107 Wiggins Road, University of Saskatchewan, SK, Canada S7N 5E5

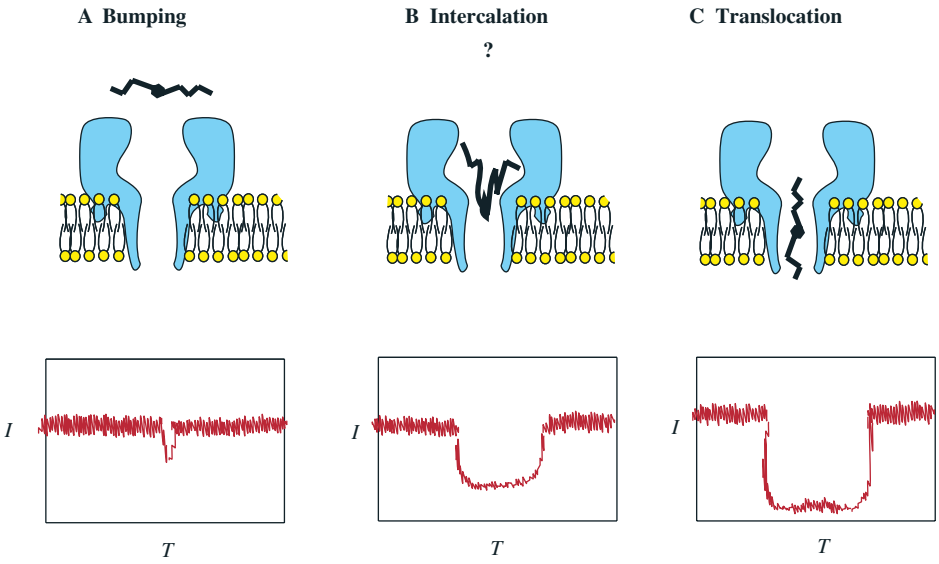

Figure 1. Types of events (top) and the corresponding event profiles (bottom). This figure is available in colour online at wileyonlinelibrary.com/journal/jpepsci.

voltage for an intercalation event but decrease for a translocation event. To test this hypothesis, a series of peptides have been prepared with increasing structural complexity.

The core 11-mer peptide has the sequence AcSRSDWDLP-GEYNH$_2$ with a net charge of −2 at pH 7.8. Addition of cysteine to the *N*-terminus or *C*-terminus gives CY12 and SC12, respectively, and addition to both termini yields CC13 (Figure 2). Two repeats of the sequence with a cysteine in the middle gives the linear peptide SY23. Peptides containing cysteine can be readily and specifically attached to a benzene tether by the displacement of bromide from bromotoluene (T1), *m*-dibromoxylene (T2), *m-tris*(bromomethyl)mesitylene (T3), and 1,2,4,5-tetrakis-(bromomethyl)benzene (T4) [30] to form molecules of increasing complexity such as CY12-T1, CY12-T2, CY12-T3, and CY12-T4 (Figure 2). It was anticipated that the more complex molecules would be unable to translocate or might 'plug the pore'. A circular molecule was also prepared, CC13-T2, by reacting CC13 with T2.

The results demonstrate that even simple peptides such as CY12-T1 and CY12-T2 can give quite complex blockade current and blockade time histograms. But since the blockade times decrease with increasing voltage, the majority of these events can be assigned to translocations. For CY12-T3 and CY12-T4, many events with a large blockade can be assigned to intercalation because the blockade time increases with increasing voltage. However, some apparent translocations are still observed. Surprisingly, the circular peptide, CC13-T2, does not translocate. In general, it is clear that it is difficult to distinguish between intercalation and translocation without detailed analysis.

Materials and Methods

Peptide synthesis

The peptides were purchased from American Peptide Company Inc. (Sunnyvale, CA). The tethered peptides were prepared as outlined in Figure 2 and described in detail by Timmeman *et al.* [30]. The tethers (T1), *m*-dibromoxylene (T2), *m-tris*(bromomethyl)-mesitylene (T3), and 1,2,4,5-tetrakis(bromomethyl)benzene (T4) were purchased from Sigma Aldrich (St. Louis, MO). They were purified by HPLC (Walters, Delta-Pak C18) and then analyzed by MALDI/TOF at the Plant Biotechnology Institute, Saskatoon. In all cases, the MH^+ was within 0.1% of the calculated value.

Peptide modeling

Molecular models were generated using *Spartan '08* version 1.2.0 (Wavefunction, Inc., Irvine, CA.). After construction of the charged molecule, the equilibrium conformer for each was found using the molecular mechanics function. This option allowed calculations to be done in an aqueous solution, and determined intramolecular interactions based on both atomic force fields and designated charges. The molecular mechanics program was permitted to either compute for a period of 30 hours on a dedicated processor (Pentium 4, 3.00 GHz, 1 GB RAM), or to examine 1000 lowest energy molecular arrangements, whichever occurred first. The most stable form of each structure is shown. Distances along *X*, *Y*, and *Z*-axes are measured using the measure distance tool within *Spartan '08.*

Lipid membrane preparation

The lipid solution, 1,2-diphytanoyl-*sn*-glycero-3-phosphocholine in $CHCl_3$, was purchased from Avanti Polar Lipids, Inc (Alabaster, AL) and dried under a vacuum for 4 h prior to experimentation. Each aliquot was stored at −20 °C until needed and redissolved in decane (Sigma Aldrich, St. Louis, MO) to a final concentration of 30 mg/ml. A basal layer of lipid was applied on the aperture of the bilayer cup (Warner Instruments, Hamden, CT) by paintbrush and excess lipid was dried under a stream of nitrogen. The bilayer cup and chamber assembly rested on an active air-floating table (Kinetic Systems, Boston, MA) inside a Faraday cage (Warner Instruments, Hamden, CT). The *cis* and *trans* compartments of the bilayer cell were filled with 1.0 ml of 1 M KCl in 10 mM potassium phosphate buffer solution (pH 7.8). The formation of the bilayer was achieved by painting the lipid solution across the aperture a second time, and was monitored by pClamp 10.1 (Axon Instruments, Union City, CA) using capacitance measurements through a pair of Ag/AgCl electrodes. Repeated brush strokes

Journal of PeptideScience

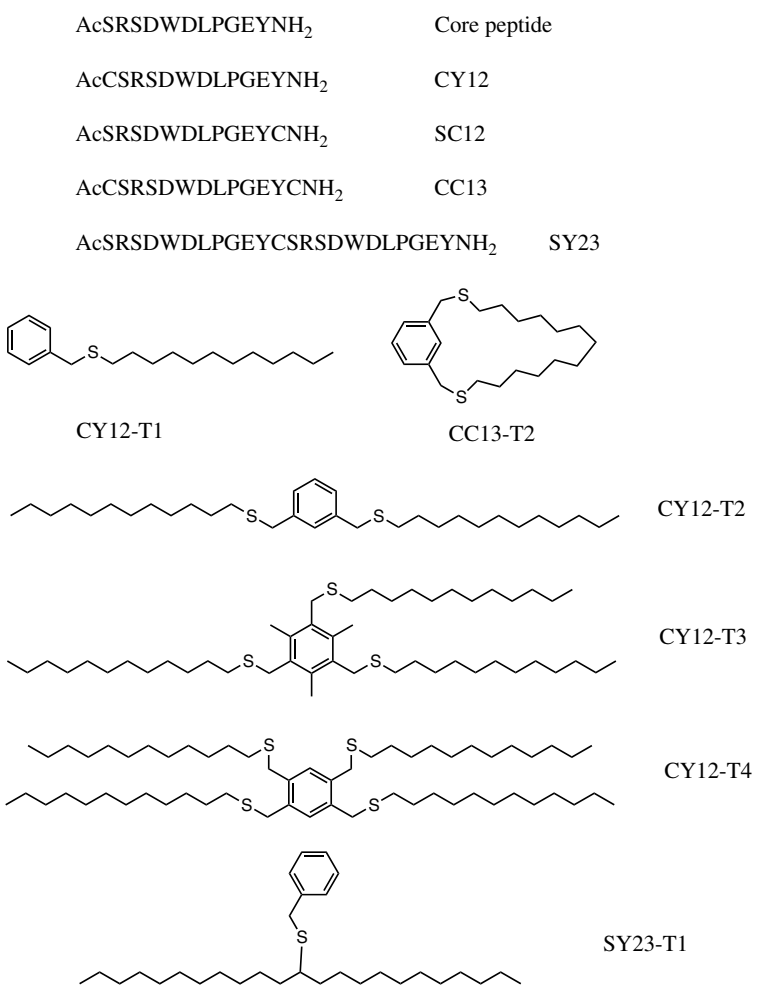

Figure 2. Sequence and structure of the peptides attached to the tethers. Each node represents an amino acid.

were needed to thin the multilayer to a thickness suitable for pore insertion, as indicated by capacitance values of ~74 pF.

Nanopore insertion

The α-hemolysin was purchased from Sigma Aldrich (St. Louis, MO). Injection of 5 µl of a 1.6 µg/ml α-hemolysin solution into the *cis* chamber adjacent to the aperture allowed for pore self-insertion and was detected by a characteristic jump in the current values. Additional α-hemolysin, in increments of 5 µl, was used if a stable pore was not achieved within 2 min of the first injection. A stable pore insertion was detected by a current jump from 0 to 100 pA per pore. Experiments were performed with up to three pores per membrane since each pore gives an identical open pore current and the event parameters for one, two, or three pores were found to be indistinguishable. Then, 5–10 µl of the 2 mg/ml sample peptide solutions were added to the *cis* chamber proximal to the aperture, giving a final peptide concentration of 0.01–0.02 mg/ml. The experiments were carried out at 22 ± 2 °C, as it was observed that the results are temperature sensitive [10].

Data collection

The bilayer experiments were run under voltage-clamp conditions using a BC-535 amplifier (Warner Instruments, Hamden, CT) connected to its corresponding Warner Instruments head stage. The transmembrane potentials that drove anions from the *cis* to the *trans* chamber were applied through a pair of Ag/AgCl electrodes. The current blockade signals were low pass-filtered at 10 kHz by an LPF-8 eight-pole Bessel filter (Warner Instruments, Hamden, CT), sampled at 100 kHz and digitized by a DigiData 1440 A digitizer (Axon Instruments, Union City, CA). The digitized data was finally recorded by a personal computer running pClamp 10.1 (Axon Instruments, Union City, CA). The programs ClampFit 10.1 (Axon Instruments, Union City, CA) and Origin 7.0 (OriginLab Corporation, Northampton, MA) were used to process all data collected [16,17,21]. Each peptide was analyzed at least twice on different membrane assemblies. In general, the measured parameters agreed to within ±1 pA and ±10% for the time, *T*. The data presented is the sum of these experiments and, therefore, represents an average.

Results

Initially, the linear peptides CY12 and SC12 and their T1 derivatives were studied. A typical current profile is shown in Figure 3, in which each spike represents an event. The blockade currents were measured for each event and assembled into histograms as described previously [21] (Figure 4). For SC12

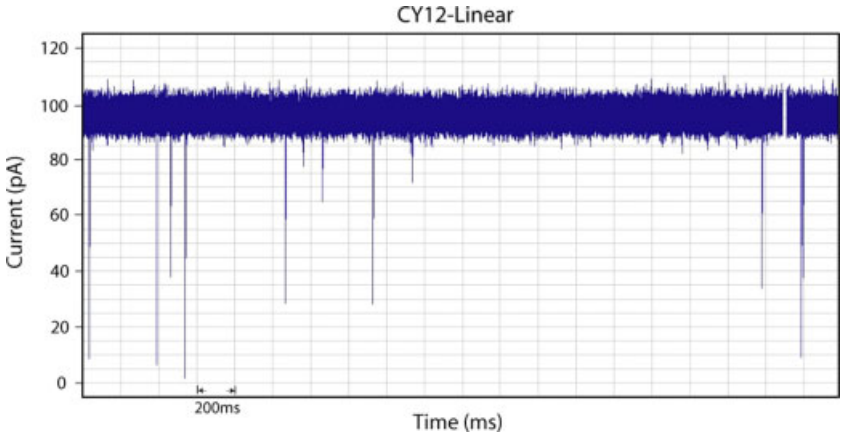

Figure 3. Event profile for CY12 covering 4 s. The open pore current is 100 pA and each spike records the change in current when a peptide interacts with the pore. This figure is available in colour online at wileyonlinelibrary.com/journal/jpepsci.

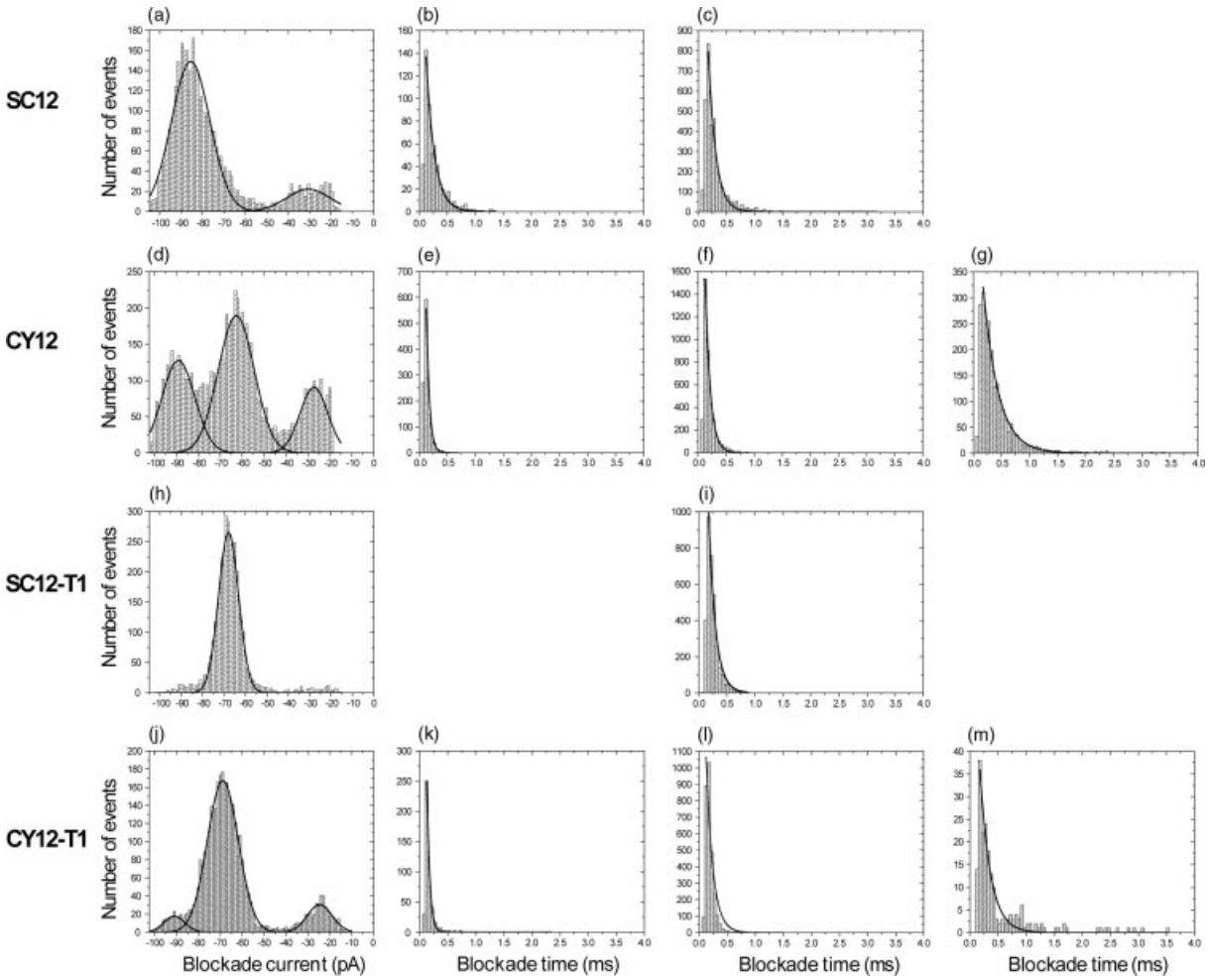

Figure 4. Blockade event histograms for the linear peptides and their T1 derivatives at −100 mV.

(Figure 4a), the blockade current histogram was analyzed as two Gaussian distributions for which the corresponding blockade time histograms are shown in Figure 4b and c. For CY12, the blockade current histogram is more complex and was fit to three Gaussian distributions (Figure 4d), for which the corresponding blockade time histograms are shown in Figure 4e–g. Similar analysis was performed for the corresponding T1 derivatives and all the blockade parameters are summarized in Table 1. [For SC12-T1 (Figure 4h), only one Gaussian distribution was used for the blockade currents because there were too few events at higher and lower currents for a meaningful analysis.] It is clear that each peptide gives a distinctive profile and that attachment of a toluene moiety causes fewer events at low current blockades and narrower distributions. In accord with previous practice, events

Journal of PeptideScience

Table 1. Event parameters, *I*, current blockade and, *T*, blockade time for the peptides of Figure 4

	I_1 (pA)	I_2 (pA)	I_3 (pA)	T_1 (ms)	T_2 (ms)	T_3 (ms)
CY12	−27[a]	−63	−89	0.05[b]	0.09	0.27
SC12	−31	−86	–	0.15	0.13	–
CY12-T1	−25	−69	−91	0.05	0.12	0.19
SC12-T1	–	−68	–	–	0.12	

[a] The error is estimated to be ±1 pA.
[b] The error is estimated to be ±10%.

with a current blockade below about −40 pA would be assigned to bumping and those above −40 pA would be translocations.

In order to provide further evidence for these assignments, the series CY12-T1, -T2, -T3, and -T4 were studied at −50, −100, and −150 mV. Typical current traces at −100 mV are shown for all four in Figure 5. For CY12-T1 and CY12-T2, simple inspection suggests that there are two broad categories, i.e. events with small current blockades between −20 and −40 pA and those above about −60 pA. The corresponding blockade current histograms are shown in Figure 6 and the parameters *I* and *T* are summarized in Table 2. In all cases, I_1 and T_1 refer to the blockade peak with the lowest blockade current, etc. (For ease of comparison, the percentage blockade currents are also listed in Table 2.) At −50 mV, CY12-T1 shows two broad Gaussian distributions (Figure 6a) but at higher voltages a third minor peak appears with a larger current blockade. The values of T_1 increase with increasing voltage and, therefore, are assigned to bumping events, whereas T_2 decreases with increasing voltage which is consistent with translocations since the peptide is negatively charged and is being driven 'downstream' by the electric potential. For both types of events, the current blockade and the proportion of bumping events increase linearly with voltage. Peak three events are difficult to assign because their frequency is low and T_3 changes little between −100 and −150 mV.

CY12-T2 has two peptide arms attached to the tether and, therefore, blockade currents and blockade times should be larger than for CY12-T1. As shown in Figure 6 and Table 2, these expectations are correct. At all voltages, the events at high blockade currents can be fit with two peaks and the values of T_2 and T_3 decrease with increasing voltage and, therefore, are assigned to translocations. As discussed below, T_3 is larger than T_2 and may be due to the translocation of folded and unfolded molecules, respectively [20]. In contrast to CY12-T1, the proportion of bumping events decreases with increasing voltage and there are two apparent bumping peaks at −150 mV.

CY12-T3 and CY12-T4 were much more difficult to analyze because, as shown in the current traces of Figure 5c and d, there were many very long blockades over 40 ms which became more frequent as the voltage was increased. Some of the blockades did not end spontaneously and had to be resolved by reversing the potential. Such events were not included in the analysis. For CY12-T3, the second peak is the largest at all voltages but the value of T_2 increases significantly with increasing voltage suggesting that these represent intercalation events rather than translocations. There is also a third small peak which is reasonably resolved at −100 and −150 mV. The value of T_3 is a maximum at −100 mV and so it is difficult to assign to either intercalation or translocation. For CY12-T4 at −150 mV, permanent blockades were so frequent that a detailed analysis could not be performed. However, even at −50 and −100 mV, bumping events predominate so that translocations, if they occur, must be rare.

Finally, blockade histograms for SY23-T1 and CC13-T2 are shown in Figure 7 with the corresponding *I* and *T* values in Table 2. Compared to CY12-T2, SY23-T1 gives only two peaks although the peaks are broader and the proportion of bumping events is

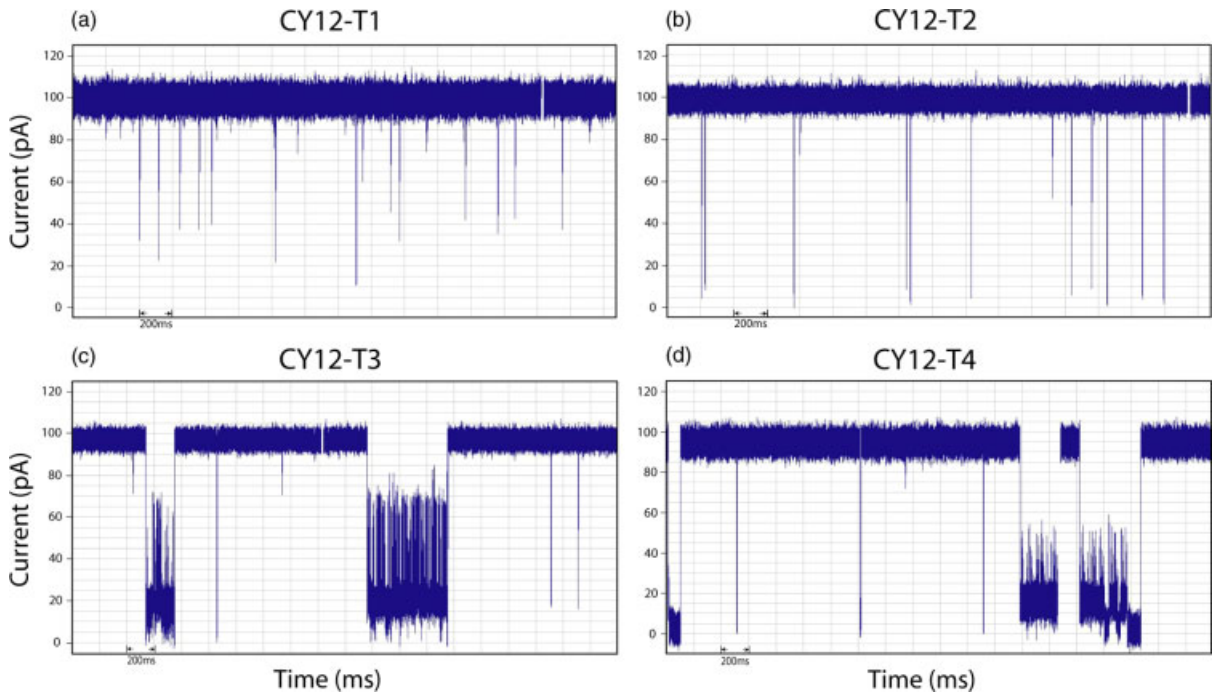

Figure 5. Current traces at −100 mV covering 4s for (a) CY12-T1,(b) CY12-T2, (c) CY12-T3, and (d) CY12-T4. This figure is available in colour online at wileyonlinelibrary.com/journal/jpepsci.

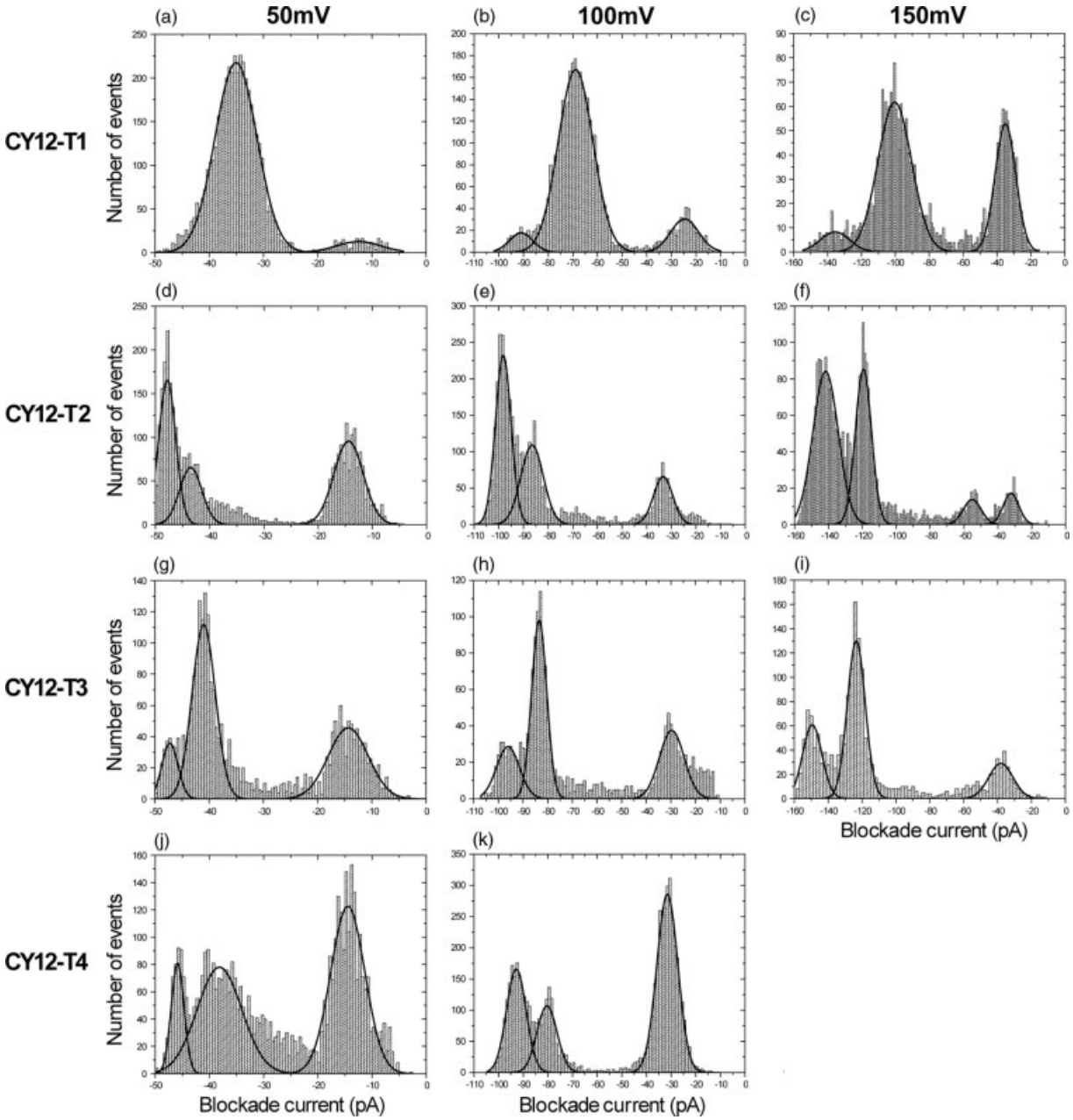

Figure 6. Blockade current histograms for CY12-T1, −2, −3, −4 at −50, −100 and −150 mV.

larger. But the value of T_2 decreases with increasing voltage again consistent with translocation. The current blockade histograms for CC13-T2 are unremarkable except that it is the only molecule for which the number of Gaussian peaks decreases from three to two as the voltage increases. On the other hand, the value of T_2 increases with increasing voltage suggesting that these are intercalation events rather than translocations.

Discussion

These experiments were initiated in an attempt to gain insights into putative protein translocation but they also provide some important details about peptide translocation. As described previously, small changes in sequence can result in large changes to the event parameters [20–25]. For example, CY12 and SC12 are identical except for the position of the cysteine at either the *N*- or *C*-terminus; yet CY12 has three peaks in the histogram of blockade current, whereas SC12 has only two and the proportion of bumping events is significantly greater for CY12. Thus, the interaction between peptide and pore is sequence dependent and partially determines the event parameters. Similarly, both CY12-T1 and SC12-T1 are distinctly different from their untethered analogs with a decrease in the proportion of bumping events in both cases. Thus, the addition of a single benzyl group which increases the hydrophobicity decreases the interaction with the outside of the pore and favors translocation. A similar effect has been observed previously upon the addition of a hydrophobic group to α-helical peptides [21]

At first sight, it might be expected that SY23-T1 and CY12-T2 would give similar results since the benzene ring is in the middle

Journal of PeptideScience

Table 2. Event parameters for the peptides of Figures 6 and 7

	Voltage (mV)	I_1 (pA)	I_2 (pA)	I_3 (pA)	T_1 (ms)	T_2 (ms)	T_3 (ms)
CY12-T1	−50	−12 (24%)[a]	−35 (70%)	–	0.01[b]	0.19	–
–	−100	−25 (24%)	−69 (69%)	−91 (91%)	0.05	0.12	0.19
–	−150	−35 (23%)	−102 (68%)	−138 (92%)	0.08	0.09	0.21
CY12-T2	−50	−14 (28%)	−43 (86%)	−48 (96%)	0.07	0.84	2.34
–	−100	−33 (33%)	−86 (86%)	−98 (98%)	0.10	0.60	1.10
–	−150	−31/55	−120 (80%)	−142 (95%)	0.05/0.19	0.37	0.59
CY12-T3	−50	−15 (30%)	−41 (82%)	−47	0.20	0.86	0.76
–	−100	−30 (30%)	−85 (85%)	−96 (96%)	0.06	2.28	1.36
–	−150	−39 (26%)	−121 (81%)	−148 (99%)	0.17	15.1	1.19
CY12-T4	−50	−14 (28%)	−38 (76%)	−47 (94%)	0.11	0.49	5.28
–	−100	−31 (31%)	−81 (81%)	−92 (92%)	0.19	1.56	2.88
SY23-T1	−50	−14 (28%)	−46 (92%)	–	0.06	1.05	–
–	−100	−35 (35%)	−90 (90%)	–	0.16	0.77	–
–	−150	−64 (43%)	−133 (89%)	–	0.44	0.45	–
CC13-T2	−50	−12 (24%)	−38 (76%)	−45 (90%)	0.03	0.09	0.18
–	−100	−22 (25%)	−75 (75%)	–	0.06	0.17	–
–	−150	−32 (21%)	−119 (79%)	–	0.09	0.50	

The numbers in brackets are the percentage blockade of the open pore current.
[a] The error is estimated to be ±1 pA.
[b] The error is estimated to be ±10%.

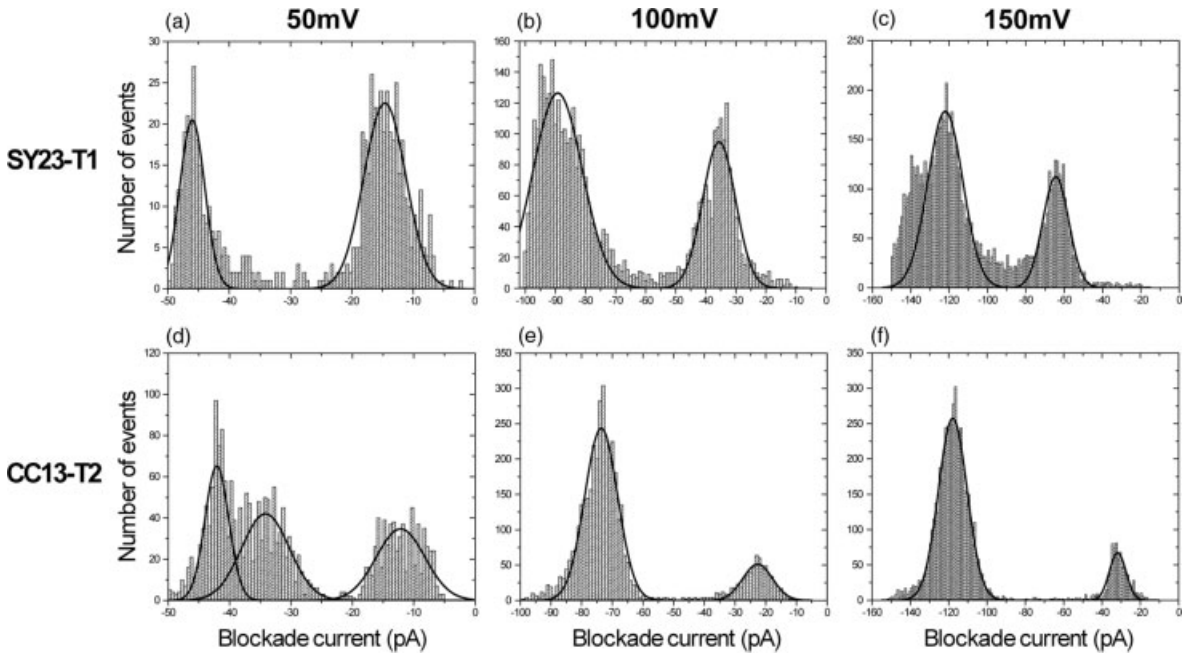

Figure 7. Blockade current histograms for SY23-T1 and CC13-T2 at −50, −100 and −150 mV.

of both peptides, but clearly this is not the case. However, for a linear conformation, the sequence of the two molecules is only identical for the *N*-terminal half so that interactions with the pore will again be different. Alternatively, folding of the molecule into a 'U- or J'-shaped conformation may be favored for one but not the other. For CY12-T2, in particular, there are two apparent translocation peaks based on the fact that T_2 and T_3 both decrease with decreasing voltage and that the percentage blockade current is roughly constant. In general, it has been observed that folded molecules give larger values of T [20]; thus the third peak for CY12-T2 is identified with folded molecules and T_2 for both CY12-T2 and SC23-T1 would be due to linear conformations. The ability of CY12-T2 to translocate in a folded or partially folded conformation is not unexpected in light of previous results with β-hairpin and collagen-like peptides [20,23]. On the other hand, for CY12-T3, there is little evidence for translocation and the majority of events appear to be intercalations. Presumably, translocation of CY12-T3 would be possible if two of the arms could fold together. However, inspection of molecular models for CY12-T3 (Supporting Information Figure S4) shows that there is considerable steric hindrance around the benzene ring and that the molecule prefers to adopt an open and extended conformation. Similarly,

molecular models for CY12-T4 (Supporting Information Figure S5) also show that the preferred conformation is star-shaped which would prevent translocation. The blockade times for CC13-T1, therefore, were most unexpected since it is a much smaller molecule, yet T_2 increases with increasing voltage. The molecular model of CY13-T2 (Supporting Information Figure S1) is globular and highly constrained with a diameter of about 2 nm which is larger than the pore (about 1.5 nm). Thus, since it cannot unfold, it cannot translocate. CY12-T1 has similar dimensions (Supporting Information Figure S2) and CY12-T2 is even larger (Supporting Information Figure S3) but they are not constrained and can unfold, allowing translocation.

From the above, it appears probable that large proteins would be unable to translocate unless completely unfolded before they entered the pore. For example, even if a partially folded protein enters the pore from one terminus, translocation would require the simultaneous threading of three strands. Unless the three strands were tightly coiled in a collagen-like helix, their diameter would be too large to pass through the small aperture of the pore [23]. Recent work with solid-state pores suggests that small proteins translocate in an unfolded conformation even though the dimensions of the pore were larger than the protein [31]. The unfolding mechanism involves the electric field at the entrance to the pore which is sufficient to pull apart amino acids of opposite charge. A similar mechanism may occur in the vestibule of the α-hemolysin pore. But, of course, CY12-T3 and CY12-T4 cannot completely unfold because they are tethered. Thus, even if one strand enters the pore, the remainder of the molecule cannot follow resulting in the observed intercalation events and permanent blockages. Another important difference between proteins and the CY peptides is the net charge density. The net charge density on the CY series of peptides is -0.17 per residue, whereas many globular proteins have net charge densities less than ± 0.05 per residue because of the presence of a central hydrophobic core. For example, maltose binding protein which translocates readily in the presence of denaturants has a net charge density of -0.02 [18]. Thus, proteins are considerably more hydrophobic and, as shown earlier, by comparison of CY12/SC12 with CY12-T1/SC12-T1, hydrophobicity favors translocation. Future experiments will be directed to studying peptides with lower charge densities.

Acknowledgements

Research funding was provided by grants to J.S.L. from NSERC and Saskatchewan Agriculture and by NSERC scholarships to H. M. and R. I. S.

Supporting information

Supporting information may be found in the online version of this article.

References

1 Song ZL, Hobaugh MR, Shustak C, Cheley S, Bayley H, Gouaux JE. Structure of staphylococcal α-hemolysin, a heptameric transmembrane pore. *Science* 1996; **274**: 1859–1866.
2 Parker MW, Buckley JT, Postma JMP, Tucker AD, Leonard K, Pattus F, Tsernoglou D. Structure of the *Aeromonas* toxin proaerolysin in its water-soluble and membrane-channel states. *Nature* 1994; **367**: 292–295.
3 Bezrukov SM. Ion channels as molecular Coulter counters to probe metabolite transport. *J. Membr. Biol.* 2000; **174**: 1–13.
4 Bayley H, Cremer PS. Stochastic sensors inspired by biology. *Nature* 2001; **413**: 226–230.
5 Martin CR, Siwy ZS. Chemistry, learning nature's way: biosensing with synthetic nanopores. *Science* 2007; **317**: 331–332.
6 Bayley H, Martin CR. Resistive-pulse sensing – from microbes to molecules. *Chem. Rev.* 2000; **100**: 2575–2594.
7 Bayley H. Sequencing single molecules of DNA. *Curr. Opin. Chem. Biol.* 2006; **10**: 628–637.
8 Rhee M, Burns MA. Nanopore sequencing technology: nanopore preparations. *Trends Biotechnol.* 2007; **25**: 174–181.
9 Branton D, Deamer DW, Marziali A, Bayley H, Benner SA, Butler T, Di Ventra M, Garaj S, Hibbs A, Huang X, Jovanovich SB, Krstic PS, Lindsay S, Ling XS, Mastrangelo CH, Meller A, Oliver JS, Pershin YV, Ramsey JM, Riehn R, Soni GV, Tabard-Cossa V, Wanunu M, Wiggin M, Schloss JA. The potential and challenges of nanopore sequencing. *Nat. Biotechnol.* 2008; **26**: 1146–1153.
10 Deamer DW, Akeson M. Nanopores and nucleic acids: prospects for ultrarapid sequencing. *Trends Biotechnol.* 2000; **18**: 147–151.
11 Meller A, Nivon L, Brandin E, Golovchenko J, Branton D. Rapid nanopore discrimination between single polynucleotide molecules. *Proc. Natl. Acad. Sci. U.S.A.* 2006; **97**: 1079–1084.
12 Kasianowicz JJ, Brandin E, Branton D, Deamer DW. Characterization of individual polynucleotide molecules using a membrane channel. *Proc. Natl. Acad. Sci. U.S.A.* 1996; **93**: 13770–13773.
13 Nakane J, Wiggin M, Marziali A. Nanosensor for transmembrane capture and identification of single nucleic acid molecules. *Biophys. J.* 2004; **87**: 615–621.
14 Tropini C, Marziali A. Multi-nanopore force spectroscopy for DNA analysis. *Biophys. J.* 2007; **92**: 1632–1637.
15 Mathe J, Visram H, Viasnoff V, Rabin Y, Meller A. Nanopore unzipping of individual DNA hairpin molecules. *Biophys. J.* 2004; **87**: 3205–3212.
16 Stefureac RI, Lee JS. Nanopore analysis of the folding of zinc fingers. *Small* 2008; **4**(10): 1646–1650.
17 Stefureac RI, Waldner L, Howard P, Lee JS. Nanopore analysis of a small 86-residue protein. *Small* 2008; **4**(1): 59–63.
18 Oukhaled G, Mathe J, Biance AL, Bacri L, Betton JM, Lairez D, Pelta J, Auvray L. Unfolding of proteins and long transient conformations detected by single nanopore recording. *Phys. Rev.* 2007; **98**: 158101–158104.
19 Long M, Cockroft SL. Biological nanopores for single molecule biophysics. *ChemBioChem* 2010; **11**: 25–34.
20 Goodrich CP, Kirmizialtin C, Huyghes-Despointes BM, Zhu A, Scholtz JM, Makarov DE, Movileanu L. Single-molecule electrophoresis of β-hairpin peptides by electrical recordings and langevin dynamics simulations. *J. Phys. Chem. B* 2007; **111**(13): 3332–3335.
21 Stefureac RI, Long Y, Kraatz HP, Howard P, Lee JS. Transport of α-helical peptides through α-hemolysin and aerolysin pores. *Biochemistry* 2006; **45**: 9172–9179.
22 Zhao Q, Jayawardhana DA, Wang D, Guan X. Study of peptide transport through engineered protein channels. *J. Phys. Chem. B* 2009; **113**: 3572–3578.
23 Sutherland TC, Long Y, Stefureac RI, Bediako-Amoa I, Kraatz H, Lee JS. Structure of peptides investigated by nanopore analysis. *Nano Lett.* 2004; **4**(7): 1273–1277.
24 Movileanu L, Schmittschmitt J, Scholtz JM, Bayley H. Interaction of peptides with a protein nanopore. *Biophys. J.* 2005; **89**: 1030–1045.
25 Zhao Q, de Zoysa RSS, Wang D, Jayawardhana DA, Guan X. Study of peptide transport through engineered protein channels. *J. Am. Chem. Soc.* 2009; **131**: 6324–6325.
26 Howorka S, Siwy Z. Nanopore analytics: sensing of single molecules. *Chem. Soc. Rev.* 2009; **38**: 2360–2384.
27 Movileanu L. Squeezing a single polypeptide through a nanoport. *Soft Matter* 2008; **4**: 925–931.
28 Movileanu L. Interrogating single proteins through nanopores: challenges and opportunities. *Trends Biotechnol.* 2009; **27**: 333–341.
29 Waring MJ. Variation of the supercoils in closed circular DNA by binding of antibiotics and drugs: evidence for molecular models involving intercalation. *J. Mol. Biol.* 1970; **54**: 247–279.
30 Timmenman P, Beld J, Puijk WC, Meloen RH. Rapid and quantitative cyclization of multiple peptide loops onto synthetic scaffolds for structural mimicry of protein surfaces. *ChemBioChem* 2005; **6**: 821–824.
31 Talaga DS, Li J. Single-molecule protein unfolding in solid state nanopores. *J. Am. Chem. Soc.* 2009; **13**: 9287–9297.

